Energy Transport in Jammed Sphere Packings

Ning Xu,[1,2] Vincenzo Vitelli,[1] Matthieu Wyart,[3] Andrea J. Liu,[1] and Sidney R. Nagel[2]
[1]*Department of Physics and Astronomy, University of Pennsylvania, Philadelphia, Pennsylvania, 19104*
[2]*The James Frank Institute, The University of Chicago, Chicago, Illinois, 60637*
[3]*HSEAS, Harvard University, Cambridge, Massachusetts, 02138*
(Received 19 June 2008; published 21 January 2009)

We calculate the normal modes of vibration in jammed sphere packings to obtain the energy diffusivity, a spectral measure of transport. At the boson peak frequency, we find an Ioffe-Regel crossover from a diffusivity that drops rapidly with frequency to one that is nearly frequency independent. This crossover frequency shifts to zero as the system is decompressed towards the jamming transition, providing unambiguous evidence of a regime in frequency of nearly constant diffusivity. Such a regime, postulated to exist in glasses to explain the temperature dependence of the thermal conductivity, therefore appears to arise from properties of the jamming transition.

DOI: 10.1103/PhysRevLett.102.038001 PACS numbers: 45.70.−n, 61.43.Fs

Zero-temperature soft-sphere models inspired by foams and granular media have given insight not only into the geometry of hard-sphere packings [1–3] but also into the physics of the low-energy excitations in glasses [4–6]. In particular, a model system of frictionless spheres interacting with finite-ranged repulsions exhibits a jamming transition (Point J) at a density corresponding to random close-packing of hard spheres [1]. At the transition, the coordination number jumps [1,7] from zero to the minimum value required for mechanical stability, the ''isostatic'' value [8,9], and there is a plateau in the density of vibrational states that extends down to zero frequency [4]. Upon compression, this plateau persists but only above a characteristic frequency, ω^*, that increases with density. The modes in the plateau region have been shown to arise from zero-frequency vibrational modes at the isostatic transition [9]. These anomalous modes are in excess of the Debye prediction and are directly connected [5,6] to excess vibrational modes in glasses, known as the ''boson peak'' [10–12]. However, it is not clear how these modes contribute to heat conduction.

In this Letter, we investigate thermal transport as a function of compression in jammed sphere packings. At the jamming threshold, we find that all delocalized modes transport heat with a low diffusivity nearly independent of frequency, in contrast to ordinary solids in which sound modes transport heat ballistically with a diverging diffusivity in the long-wavelength limit. The behavior at Point J is reminiscent of many amorphous solids, which unlike crystals, display a thermal conductivity that rises monotonically with temperature T [13]. This property has been posited to arise from a frequency regime of small, constant diffusivity [14–16]. We show that this regime can originate from the vibrational spectrum at Point J. Upon compression, the low-diffusivity modes persist, but only above a crossover frequency corresponding to the frequency of the boson peak, ω^* [17,18]; below ω^*, the spectrum is dominated by transverse plane waves.

Our model [1,4] is a 50/50 mixture of spheres with a diameter ratio of 1.4. Particles i and j interact in 3 dimensions via a one-sided harmonic potential: $U(r_{ij}) = \frac{\epsilon}{2}(1 - r_{ij}/\sigma_{ij})^2$ when the distance between their centers, r_{ij}, is less than the sum of their radii, σ_{ij} and zero otherwise. Jammed packings at $T = 0$ are obtained by conjugate-gradient energy minimization. We study systems of $250 \leq N \leq 10,000$ particles with periodic boundary conditions. The packing fraction at the onset of jamming, ϕ_c, is characterized by the onset of a nonzero pressure. We determine ϕ_c and obtain $T = 0$ configurations at controlled $\Delta\phi \equiv \phi - \phi_c$ as in Ref. [4]. For each configuration, we diagonalize its Hessian matrix [19], whose m^{th} eigenvalue is the squared frequency, ω_m^2, of the orthonormal eigenmode described by the displacement $\vec{e}_m(j)$ of each particle j. The particle mass, M, interaction energy, ϵ, and diameter of the smaller particle, σ, are set to unity. The frequency is in units of $\sqrt{\epsilon/M\sigma^2}$.

We also study an ''unstressed'' model in which we use energy-minimized configurations obtained from the previous model, and replace the interaction potential $U(r_{ij})$ between each pair of overlapping particles with an unstretched spring with the same stiffness, $U''(r_{ij})$. Because all springs are unstretched, there are no forces between particles in their equilibrium positions so that stable configurations for the stressed system are also stable in the unstressed one. This corresponds to dropping terms depending on U' in the Hessian [8,9].

For a strongly scattering system, a diffusive description of energy transport can be more useful than one in terms of ballistic propagation with a very short mean-free path. Therefore, instead of calculating the thermal conductivity, $\kappa(T)$, using molecular dynamics [20,21], we calculate the thermal diffusivity, $d(\omega_m)$ for vibrational mode m [15,16].

$\kappa(T)$ can be expressed in terms of $d(\omega_m)$ and the heat capacity $C(\omega_m)$ [15,16,22]:

$$\kappa(T) = \frac{1}{V}\sum_m C(\omega_m)d(\omega_m) = \frac{1}{V}\int_0^\infty d\omega D(\omega)C(\omega)d(\omega), \tag{1}$$

where the sum is over all normal modes m, V is the system volume, and $D(\omega) \equiv \sum_m \delta(\omega_m - \omega)$ is the density of vibration modes. Thus, $C(\omega) = k_B(\beta\hbar\omega)^2 e^{\beta\hbar\omega}/(e^{\beta\hbar\omega} - 1)^2$ (where $\beta \equiv 1/k_B T$ and k_B is the Boltzmann constant) depends on T and characterizes the heat carried at frequency ω. $d(\omega)$ is a T-independent scattering function.

The physical meaning of diffusivity is best illustrated operationally. Consider a wave packet narrowly peaked at ω and localized at $\vec{r}$ at time $t = 0$. Over time, the wave packet spreads out and can be characterized by a time-independent diffusivity given by the square of the width of the wave packet at time t, divided by t [15]. In a weakly scattering system, $d(\omega) = c\ell(\omega)/3$, where c is the sound speed and $\ell(\omega)$ the phonon mean-free path.

We follow Allen and Feldman [16] to calculate $d(\omega)$ in terms of the normal modes of a given configuration, using the Kubo-Greenwood formula for the thermal conductivity as the response to a temperature gradient that couples different modes. We use

$$d(\omega) = \frac{\pi}{12M^2\omega^2}\int_0^\infty d\omega' D(\omega') \times \frac{(\omega + \omega')^2}{4\omega\omega'}|\vec{\Sigma}(\omega, \omega')|^2\delta(\omega - \omega') \tag{2}$$

where the vector heat-flux matrix elements are

$$|\vec{\Sigma}(\omega, \omega')|^2 = \frac{\sum_{mn}|\vec{\Sigma}_{mn}|^2\delta(\omega - \omega_m)\delta(\omega' - \omega_n)}{D(\omega)D(\omega')} \tag{3}$$

where m and n index the vibrational modes.

For a finite system the modes are discrete. We calculate the matrix elements $\vec{\Sigma}_{mn}$ from the Hessian $H^{ij}_{\alpha\beta}$ and its m^{th} normalized eigenvector $e_m(i;\alpha)$ [16] via

$$\vec{\Sigma}_{mn} = \sum_{ij,\alpha\beta}(\vec{r}_i - \vec{r}_j)e_m(i;\alpha)H^{ij}_{\alpha\beta}e_n(j;\beta), \tag{4}$$

where $\{i, j\}$ and $\{\alpha, \beta\}$ label particles and their Cartesian coordinates, respectively.

In a finite system, the delta function in Eq. (2) must be replaced by a representation with nonzero width, η. We use [16] $g(\omega_m - \omega_n, \eta) = \eta/\{\pi[(\omega_m - \omega_n)^2 + \eta^2]\}$ and define

$$d(\omega_m, \eta, N) \equiv \frac{\pi}{12M^2\omega_m^2}\sum_{n\neq m}\frac{(\omega_m + \omega_n)^2}{4\omega_m\omega_n} \times |\vec{\Sigma}_{mn}|^2 g(\omega_n - \omega_m, \eta). \tag{5}$$

We set $\eta = \gamma\delta\omega$, where $\gamma > 1$ and $\delta\omega$ is the average spacing between successive modes. The desired $d(\omega)$ is then $d(\omega, \eta, N)$ in the double limit $N \to \infty$, $\eta \to 0^+$.

We use Eqs. (2)–(5) to calculate the diffusivity. Our goal is to extract $d(\omega)$ for an infinite system so we must confront finite-size effects. We will show that $|\vec{\Sigma}|^2$ has a particularly simple form at the jamming threshold, enabling us to determine the $N \to \infty$ behavior.

Figure 1(a) shows the matrix elements $|\vec{\Sigma}(\omega, \omega')|^2$ defined in Eq. (3) for packings at $\phi - \phi_c = 10^{-6}$ for different values of ω versus ω'. Figure 1(b) shows that all the curves can be collapsed for different system sizes, N, and frequencies, ω, except at high ω' where the modes are localized [23–25]. The inset to Fig. 1(b) shows that the scale factors satisfy $s^2 = \omega^2$ and $w = \omega$, except at high ω for localized states. The data collapse demonstrates that the only noticeable system-size dependence is a prefactor of $1/N$. Since for large N, the density of states scales as N [4], Eq. (2) therefore yields a well-defined diffusivity in the $N \to \infty$ limit [solid curve in Fig. 1(c)].

Note that the collapse in Fig. 1(b) implies that $|\vec{\Sigma}(\omega, \omega)|^2 \propto \omega^2/N$ at low frequencies. This scaling arises when overlap with nearby modes, described by Eq. (4), is small and independent of frequency and when modes are spatially uncorrelated [26]. Thus, Eq. (2) implies that $d(\omega) \propto D(\omega)$ at low ω. At Point J, because the density

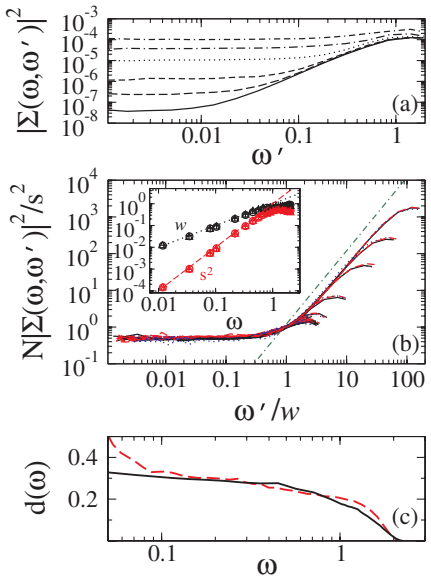

FIG. 1 (color online). Diffusivity at $\Delta\phi = 10^{-6}$. (a) Heat-flux matrix elements $|\Sigma(\omega, \omega')|^2$ plotted versus ω' at $N = 2000$ for $\omega = 0.012$ (solid line), 0.035 (long dashed line), 0.08 (short dashed line), 0.10 (dotted line), 0.22 (dot-dashed line), and 0.68 (dot-dash-dashed line). (b) Plot showing collapse of $|\Sigma(\omega, \omega')|^2$ at $N = 2000$ (black solid line), 1000 (red dashed line), and 500 (blue dotted line) with scale factors s^2 and w. The green dot-dashed line has a slope of 2. Inset: Scale factors s^2 (red symbols) and w (black symbols) versus ω. We find $s^2 \propto \omega^2$ (red dashed line) and $w \propto \omega$ (black dotted line) except at high ω. (c) Plot of $d(\omega, \eta = 0.002, N = 2000)$ defined in Eq. (5) (dashed line). Solid line: predicted $d(\omega)$ for $N \to \infty$.

of states is nearly constant down to $\omega = 0$ [4], the diffusivity is nearly constant as well. [The small slope of $d(\omega)$ with frequency is due to the slight ω dependence of $D(\omega)$.] These results show that although the low-frequency modes are extended at the jamming threshold [24], they do not behave like plane waves, and the usual divergence of diffusivity is completely suppressed.

Over most of the frequency range, this $N \to \infty$ prediction agrees well with the dashed curve in Fig. 1(c), which shows $d(\omega, \eta, N)$ for a finite system. However, at low ω, $d(\omega, \eta, N)$ has an upturn; this upturn is a finite-size artifact that can be shown from Eqs. (2)–(5) to scale as ω^{-3} with a prefactor that vanishes as $N \to \infty$, $\eta \to 0$ [26].

We now study diffusivity for systems compressed beyond the jamming threshold. The data for the unstressed model are particularly simple to interpret. In this case, the system is always held at zero pressure, so that increasing $\Delta\phi \equiv \phi - \phi_c$ corresponds to increasing only the average coordination number in the network. At all compressions, Fig. 2(a) shows that $d(\omega, \eta = 0.002, N = 2000)$ vanishes at high ω for localized modes. At low ω, there is the upturn due to finite-size effects discussed above; this upturn lies at frequencies below those shown in Fig. 2. At intermediate ω, the diffusivity decreases rapidly with increasing ω until it reaches a small constant value d_0 for $\omega > \omega_d$. Below ω_d, the modes are discrete due to the finite system size, as indicated by the discrete points in Fig. 2(a). The mode

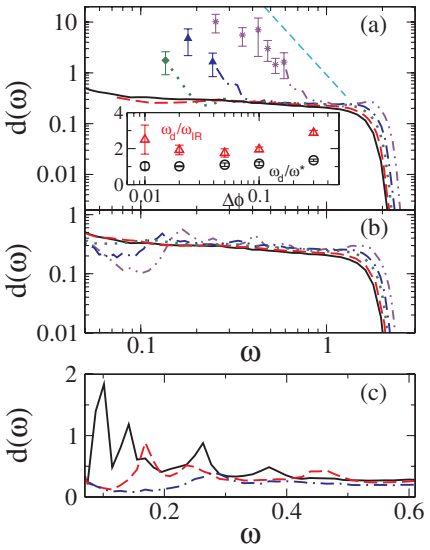

FIG. 2 (color online). Diffusivity versus compression. $d(\omega, \eta = 0.002, N = 2000)$ for the (a) unstressed and (b) stressed systems at $\Delta\phi = 10^{-6}$ (solid black line), 0.01 (red dashed line), 0.05 (green dotted line), 0.1 (blue dot-dashed line), and 0.3 (purple dot-dot-dashed line). In (a), the cyan dashed line indicates a power-law of ω^{-4} and the closed symbols indicate the degenerate sets of discrete plane-wave modes in our finite system. Inset: The ratios ω_d/ω^* (open circles) and $\omega_d/\omega_{\mathrm{IR}}$ (open triangles) versus $\Delta\phi$. (c) $d(\omega, \eta = 0.004, N)$ for the stressed system at $\Delta\phi = 0.5$ for $N = 10,000$ (black solid line), 2000 (red dashed line), and 500 (blue dot-dashed line).

frequencies correspond to $\omega = c_T k_n$, where c_T is the transverse sound speed and k_n are the lowest allowed wave vectors. The calculated diffusivity below ω_d decreases sharply with increasing ω as expected for scattering of plane waves [22]. Thus, ω_d marks the crossover from transverse plane waves to a small, nearly constant diffusivity.

The frequency ω_d can be understood as the Ioffe-Regel crossover from weak to strong scattering of transverse modes [27]. For $\omega < \omega_d$, the transverse plane waves obey $\omega = c_T k$, where k is the wave vector. As ω approaches ω_d, we have shown $d(\omega) = c_T \ell/3 \to d_0$, where ℓ is the phonon scattering mean-free path. The Ioffe-Regel criterion, $k\ell \approx 1$, predicts a crossover frequency near $\omega_{\mathrm{IR}} \equiv c_T^2/3d_0$. For our harmonic system, the transverse speed $c_T \propto \Delta\phi^{0.25}$ [1] so that $\omega_{\mathrm{IR}} \propto \Delta\phi^{0.5}$. The inset to Fig. 2 indeed shows for transverse modes, $\omega_d/\omega_{\mathrm{IR}} \approx 2$ over our range of compression, consistent with the Ioffe-Regel criterion.

Figure 2(a) (inset) also shows the ratio of ω_d to the boson peak frequency, ω^*, defined as the onset frequency for the plateau in the density of states, which was previously shown to scale as $\Delta\phi^{0.5}$ [4,5]. The ratio ω_d/ω^* is constant over a wide range of $\Delta\phi$. Studies of silica [28,29] and several disordered models [17,18] observe that the boson peak frequency and Ioffe-Regel crossover frequency agree within a factor of order unity. In our system, this relation is unambiguous because both frequencies shift together as $\Delta\phi$ is varied. Our results also indicate that at Point J, $\omega_d \to 0$ and $d(\omega)$ should remain nearly flat down to zero frequency, as shown independently in Fig. 1(c). Therefore, the modes above ω_d (i.e., those with constant diffusivity) can be identified as the anomalous modes that derive from soft modes at the isostatic point [9,6].

While the unstressed system may be appropriate for systems where the coordination at threshold exceeds the isostatic value (such as frictional systems [30]), we are also interested in systems where interparticle forces increase with $\Delta\phi$. These forces lower both the sound speed c_T which controls the Ioffe-Regel crossover frequency [1] and the frequencies of modes in the plateau [9]. Finite-size effects, which cut off plane waves at low ω, are therefore more obstructive in stressed systems.

Figure 2(b) shows that there is no discernible change in the diffusivity of the stressed system over the range $10^{-6} \leq \Delta\phi \leq 10^{-2}$. Above $\Delta\phi \approx 10^{-2}$, structure develops at intermediate frequencies. Each peak can be identified with one of the first few allowed wave vectors for longitudinal or transverse modes [26]. Figure 2(c) shows that as N increases, the plane-wave peaks shift to lower frequencies and grow closer together, as expected, so that for high enough N, peaks in a given frequency range will merge into a smooth curve as peak widths exceed their spacing. We therefore conclude that this structure will disappear in the infinite-size limit when the only observable plane-wave peaks will be shifted to zero frequency.

Figure 2(c) also shows that at frequencies below some ω_d, the peak heights increase with N and decreasing ω, suggesting that the diffusivity rises smoothly with decreasing ω in the thermodynamic limit. Above ω_d, $d(\omega) = d_0$, a constant. In the unstressed case, we found plane-wave behavior below $\omega_d \sim \omega_{\mathrm{IR}} = c_T^2/3d_0$. In the stressed case, we speculate that ω_d might be similarly defined and should also increase with $\Delta\phi^{0.5}$ since $c_T \propto \Delta\phi^{0.25}$ for stressed as well as unstressed cases [1].

At the jamming threshold, we can calculate the thermal conductivity, $\kappa(T)$, from Eq. (1), and obtain a finite answer even within the harmonic approximation because the diffusivity does not diverge at low ω. By setting $d(\omega)$ and $D(\omega)$ to be constant up to the localization threshold, we find $\kappa \propto T$ up to the Debye temperature. At high T, κ saturates when all modes are excited.

One of the most striking differences between heat conduction in ordered and disordered structures is that the thermal conductivity κ of crystalline materials first rises with increasing T but eventually drops due to phonon-phonon scattering [13], while κ for glasses increases monotonically in T. This perplexing property of glasses has been explained heuristically by assuming that phonons are scattered so strongly by structural disorder that transport becomes diffusive, with a frequency regime of small, constant thermal diffusivity [14–16]. In our finite-sized unstressed systems, we see clear evidence for such a regime of nearly constant diffusivity, and find that its frequency onset, given by the Ioffe-Regel crossover for transverse phonons, increases with compression. Anharmonic effects could also contribute to κ but are not needed to produce this regime of nearly constant diffusivity. For the compressed system with stress, our results are much less clear in the low-ω regime because of finite-size effects. However, above some intermediate frequency, we again find a constant diffusivity and constant density of states, which lead to the rise in the thermal conductivity as in the unstressed case.

In earlier work, we showed that the vibrational spectra of model systems such as the Lennard-Jones glass could be understood in terms of jammed sphere packings [5,6]. We now find that these packings capture some of the crucial physics invoked to explain the temperature dependence of the thermal conductivity–a crossover from low-ω transverse phonons to excess vibrational modes of nearly constant diffusivity [17]. The physical origin of the diffusive modes lies in the behavior of packings at the jamming threshold, where the Ioffe-Regel crossover frequency vanishes. Upon compression, the flat diffusivity shifts to higher frequencies but does not disappear. Thus, compressed sphere packings are a useful starting point for understanding energy transport in glasses.

We thank W. Ellenbroek, R. D. Kamien, T. C. Lubensky, Y. Shokef, and T. A. Witten for helpful discussions. This work was supported by DE-FG02-05ER46199 (A. L., N. X., and V. V.), DE-FG02-03ER46088 (S. N. and N. X.), NSF-DMR05-47230 (V. V.), and NSF-DMR-0213745 (S. N.).

[1] C. S. O'Hern, L. E. Silbert, A. J. Liu, and S. R. Nagel, Phys. Rev. E **68**, 011306 (2003).
[2] A. Donev, S. Torquato, and F. H. Stillinger, Phys. Rev. E **71**, 011105 (2005).
[3] L. E. Silbert, A. J. Liu, and S. R. Nagel, Phys. Rev. E **73**, 041304 (2006).
[4] L. E. Silbert, A. J. Liu, and S. R. Nagel, Phys. Rev. Lett. **95**, 098301 (2005).
[5] N. Xu, M. Wyart, A. J. Liu, and S. R. Nagel, Phys. Rev. Lett. **98**, 175502 (2007).
[6] M. Wyart, Ann. Phys. (Paris) **30**, 1 (2005).
[7] D. J. Durian, Phys. Rev. Lett. **75**, 4780 (1995).
[8] S. Alexander, Phys. Rep. **296**, 65 (1998).
[9] M. Wyart, S. R. Nagel, and T. A. Witten, Europhys. Lett. **72**, 486 (2005); M. Wyart, L. E. Silbert, S. R. Nagel, and T. A. Witten, Phys. Rev. E **72**, 051306 (2005).
[10] A. P. Sokolov, U. Buchenau, W. Steffen, B. Frick, and A. Wischnewski, Phys. Rev. B **52**, R9815 (1995).
[11] S. N. Taraskin and S. R. Elliott, Phys. Rev. B **59**, 8572 (1999).
[12] V. L. Gurevich, D. A. Parshin, and H. R. Schober, Phys. Rev. B **67**, 094203 (2003).
[13] R. O. Pohl, X. Liu, and E. Thompson, Rev. Mod. Phys. **74**, 991 (2002).
[14] C. Kittel, Phys. Rev. **75**, 972 (1949).
[15] P. Sheng and M. Zhou, Science **253**, 539 (1991).
[16] P. B. Allen and J. L. Feldman, Phys. Rev. Lett. **62**, 645 (1989); P. B. Allen and J. L. Feldman, Phys. Rev. B **48**, 12581 (1993); J. L. Feldman, P. B. Allen, and S. R. Bickham, *ibid.* **59**, 3551 (1999).
[17] H. Shintani and H. Tanaka, Nature Mater. **7**, 870 (2008).
[18] D. A. Parshin and C. Laermans, Phys. Rev. B **63**, 132203 (2001).
[19] For large systems, we use ARPACK: http://www.caam.rice.edu/software/ARPACK.
[20] P. Jund and R. Jullien, Phys. Rev. B **59**, 13707 (1999).
[21] P. Sheng, M. Zhou, and Z. Q. Zhang, Phys. Rev. Lett. **72**, 234 (1994).
[22] S. John, H. Sompolinsky, and M. J. Stephen, Phys. Rev. B **27**, 5592 (1983); W. Schirmacher, Europhys. Lett. **73**, 892 (2006).
[23] S. R. Nagel, A. Rahman, and G. S. Grest, Phys. Rev. Lett. **47**, 1665 (1981).
[24] L. E. Silbert, A. J. Liu, and S. R. Nagel, arXiv:0803.2696.
[25] Z. Zeravcic, W. van Saarloos, and D. R. Nelson, Europhys. Lett. **83**, 44001 (2008).
[26] V. Vitelli, N. Xu, M. Wyart, A. J. Liu, and S. R. Nagel (to be published).
[27] A. F. Ioffe and A. R. Regel, Prog. Semicond. **4**, 237 (1960).
[28] E. Rat, M. Foret, E. Courtens, R. Vacher, and M. Arai, Phys. Rev. Lett. **83**, 1355 (1999); B. Rufflé, D. A. Parshin, E. Courtens, and R. Vacher, Phys. Rev. Lett. **100**, 015501 (2008).
[29] J. Horbach, W. Kob, and K. Binder, Eur. Phys. J. B **19**, 531 (2001).
[30] E. Somfai, M. van Hecke, W. G. Ellenbroek, K. Shundyak, and W. van Saarloos, Phys. Rev. E **75**, 020301(R) (2007).